ISSN 0252-1075

Research Report No.RR-059

Contributions from

Indian Institute of Tropical Meteorology

Evaluation of a limited area model forecasts

By

S.S.Singh, S.S.Vaidya, A.Bandyopadhyay, A.A.Kulkarni,
S.M.Bawiskar, J.Sanjay, D.K.Trivedi & Usha Iyer

PUNE-411 008
INDIA

OCTOBER 1994

Evaluation of a limited area model forecasts

S.S.Singh, S.S.Vaidya, A.Bandyopadhyay,

A.A.Kulkarni,S.M.Bawiskar,J.Sanjay,

D.K.Trivedi and Usha Iyer

Indian Institute of Tropical Meteorology,

Pashan, Pune-411008, India

Abstract

A 3-day forecasts of a limited area model for 31 successive initial states of July 1979 have been evaluted to investigate the potential application value of the model for short range monsoon prediction over Indian region. The forecast wind fields are averaged over the month of July 1979 for different forecast intervals (viz., 1-day, 2-day and 3-day) and compared with the analysis. A number of verification statistics relevant to short range prediction is also computed and presented.

1. Introduction

A limited area model was formulated and tested by Singh et al. (1990) for short range prediction of monsoon depression. Rajagopal and Singh (1991) incorporated the improved lateral boundary conditions and modified Kuo convection scheme in the model. These experiments were done for a case of monsoon depression of Indian summer monsoon of 1979. Subsequently, the resolution in the vertical was increased from six to nine levels and the model top (p_t) was placed at p_t=0 hPa instead of p_t=100 hPa.

In the present study,the model with increased vertical resolution

was run for a 3-day forecast with 31 successive initial states of 1-31 July 1979. A number of verification statistics has been computed for 1-day, 2-day and 3-day mean forecast fields to investigate application potential value of the model for short range monsoon prediction over Indian region.

2. Data

The FGGE IIIb data of 12 GMT 1-31 July 1979 were used as 31 successive initial states to the model. The chief synoptic features during July 1979 are the following :

The monsoon set in on 11 June over the southern tip of the country and by 15 July the monsoon covered the entire country. Drought conditions prevailed over North and Central India and the monsoon was weak over most parts of the country during the first and 3rd week of July. There was a break in monsoon from 17-23 July. The rainfall for the month of July was deficient and in general, 1979 was a deficient monsoon year.

3. Model

A nine-level primitive equation model in a (x,y,σ,t) coordinate system has been used for the present study.

Model Equations :

The model equations are in sigma coordinate and are in flux form. The σ is defined as,

$$\sigma = \frac{p - p_t}{p_s - p_t}$$

The $p_s - p_t$ is denoted as π. The pressure p at any point on σ

level is related with π as follows

$$p=\sigma\pi+p_t$$

The set of model equations are as follows :

Momentum Equations

$$\frac{\partial}{\partial t}\left(\frac{\pi}{m^2}u\right)=-\frac{\partial}{\partial x}(u^*u)-\frac{\partial}{\partial y}(v^*u)-\frac{\partial}{\partial\sigma}\left(\frac{\pi}{m^2}\dot{\sigma}u\right)+\frac{\pi}{m^2}v\left[f-v\frac{\partial m}{\partial x}+u\frac{\partial m}{\partial y}\right]-\frac{\pi}{m}\frac{\partial\phi}{\partial x}$$

$$-C_p\frac{\pi\theta}{m}\frac{\partial P^\kappa}{\partial x}+\frac{\pi}{m^2}F_u-\frac{g}{m^2}\left(\frac{\partial\tau}{\partial\sigma}\right)_x$$

$$\frac{\partial}{\partial t}\left(\frac{\pi}{m^2}v\right)=-\frac{\partial}{\partial x}(u^*v)-\frac{\partial}{\partial y}(v^*v)-\frac{\partial}{\partial\sigma}\left(\frac{\pi}{m^2}\dot{\sigma}v\right)+\frac{\pi}{m^2}u\left[f-v\frac{\partial m}{\partial x}+u\frac{\partial m}{\partial y}\right]-\frac{\pi}{m}\frac{\partial\phi}{\partial y}$$

$$-C_p\frac{\pi\theta}{m}\frac{\partial P^\kappa}{\partial y}+\frac{\pi}{m^2}F_v-\frac{g}{m^2}\left(\frac{\partial\tau}{\partial\sigma}\right)_y$$

Thermodynamic Energy Equation

$$\frac{\partial}{\partial t}\left(\frac{\pi}{m^2}\theta\right)=-\frac{\partial}{\partial x}(u^*\theta)-\frac{\partial}{\partial y}(v^*\theta)-\frac{\partial}{\partial\sigma}\left(\frac{\pi}{m^2}\dot{\sigma}\theta\right)+\frac{\pi}{m^2}F_T+\frac{\pi}{m^2}D_T+\frac{g}{C_p}\frac{1}{m^2}\frac{1}{P^\kappa}\frac{\partial H}{\partial\sigma}$$

Equation for water vapour

$$\frac{\partial}{\partial t}\left(\frac{\pi}{m^2}q\right)=-\frac{\partial}{\partial x}(u^*q)-\frac{\partial}{\partial y}(v^*q)-\frac{\partial}{\partial\sigma}\left(\frac{\pi}{m^2}\dot{\sigma}q\right)+\frac{\pi}{m^2}F_q+\frac{\pi}{m^2}M+\frac{g}{m^2}\frac{\partial E}{\partial\sigma}$$

Continuity Equation

$$\frac{\partial}{\partial t}\left(\frac{\pi}{m^2}\right)=-\frac{\partial u^*}{\partial x}-\frac{\partial v^*}{\partial y}-\frac{\partial}{\partial\sigma}\left(\frac{\pi\dot{\sigma}}{m^2}\right)$$

$\dot{\sigma}$ Equation

$$\left(\frac{\pi\dot{\sigma}}{m^2}\right)_\sigma=\left(\frac{\pi\dot{\sigma}}{m^2}\right)_{\sigma+\Delta\sigma}+\int_\sigma^{\sigma+\Delta\sigma}\left[\frac{\partial}{\partial t}\left(\frac{\pi}{m^2}\right)+\frac{\partial u^*}{\partial x}+\frac{\partial v^*}{\partial y}\right]d\sigma$$

Hydrostatic Equation

$$\frac{\partial \phi}{\partial \sigma} = -C_p \theta \frac{\partial P^{\kappa}}{\partial \sigma}$$

where,

$$u^* = \frac{u\pi}{m} \quad , \quad v^* = \frac{v\pi}{m} \quad , \quad \kappa = \frac{R}{C_p} \quad , \quad P = \frac{p}{1000}$$

In vertical,between sigma equal to 0 and 1 there are nine model sigma levels(.97,.92,.85,.70,.50,.30,.145,.07,.025). The wind components, mixing ratio, potential temperature and geopotential height are defined at these levels. The vertical-σ velocity ($\dot{\sigma}$)is defined at intermediate levels. (Fig.1) shows the vertical structure of the model. The variables are staggerred in horizontal and in vertical. Arakawa B-type of staggering is used that is wind components are defined at the centre of the grid and other variables at the corner of the grid lattice (Fig.2) The horizontal grid of 150 km on Mercator projection is used. The horizontal domain extends from 10^{O}S to 40^{O}N and 45^{O}E to 120^{O}E. Mass, energy, potential temperature and variance of potential temperature conserving finite difference scheme (Arakawa and Mintz, 1974) for space derivatives is used. For time integration, economic explicit scheme following (Tatsumi, 1983)is used. In vertical $\dot{\sigma} = 0$ at $\sigma = 1$ and at $\sigma = 0$ and a horizontal tendency modification scheme following Perkey and Kreitzberg (1976) is used for lateral boundary conditions. The model physics includes the large scale precipitation, Kuo (1974) type of cumulus convection, dry convective adjustment,

the horizontal diffusion, the sensible heat supply ,evaporation over the sea and the smooth orography. A simple scheme of adjusting the divergence in a vertical column following Sasaki et al. (1979) based on variational adjustment of horizontal wind components has been applied to suppress the external gravity waves in the initial data.

The horizontal diffusion in the model is parameterized using a fourth order Laplacian formulation with constant diffusion coefficients ($K=10^5$ m^2 s^{-1}). The surface fluxes of momentum,heat and moisture are evaluated using bulk aerodynamic formulae with the bulk coefficients over sea estimated following Kondo (1975) as a function of stability. The bulk coefficients over land are assumed constant (C_D =0.0043). Surface fluxes of heat and moisture are not evaluated over land in the model. The vertical diffusion of heat, moisture and momentum are computed using the K-theory. The diffusion coeffients are determined from the mixing length theory as a function of vertical shear and stability. At the bottom of the model atmosphere the fluxes are assumed to be similar to the surface fluxes whereas at the top of the PBL the fluxes are set to zero.The cumulus parameterization scheme used in the model is according to the Kuo scheme. It is considered that the cumulus convection always occurs in region of deep layers of conditionally unstable stratification over areas of mean low level convergence and that the vertical profiles of temperature and humidity inside the cloud follow those of a moist adiabat.Kuo(1974) introduced a division of the convergence of moisture into a fraction bM_t of the total which

increases the humidity of the air,and a fraction $(1-b)M_t$,which is condensed and precipitates as rain or is carried away with the latent heat warming the air.Kuo suggested that b would be much less than one in regions of low level convergence in the tropics, but leaves its evaluation to empirical data. Anthes(1977) proposed that b depend on the mean relative humidity of the air in such a way that moistening is greater when the air is drier. This formulation for b is used in the model. Large scale condensational heating is simulated in the model by removal of supersaturation whenever it is encountered in the model prediction. Condensed moisture is assumed to fall down to ground as precipitation without evaporation. Whenever superadiabatic lapse rates are encountered, by performing Dry Convective Adjustment the superadiabatic lapse rate is brought back to dry adiabatic lapse rate conserving the dry static energy.

4. Results and discussion

The model forecasts are interpolated from sigma to the standard pressure levels . The results are presented at the standard pressure levels.

4.1 Wind field

The mean forecast wind charts at 850 and 200 hPa levels for 1-day, 2-day and 3-day forecasts are prepared and shown in Fig.3. These are verified against the mean observed wind for the month of July 1979 (Fig. 3).

a. Observed wind

At 850 hPa level, (Fig. 3a) cyclonic circulation is seen

over NW India and adjoining Pakistan. To the west of this cyclonic circulation, wind speeds are 10-20 knots and in the remaining northern part of the domain, the wind strength is 5-10 knots. The trough associated with this cyclonic circulation extends from NW India upto Head Bay. The cross- equatorial flow and the anticyclone are seen along the equator. The strength of the low level jet over Arabian sea is 30-40 knots and that of the cross-equatorial flow is 10-20 knots.

The 200 hPa level (Fig. 3e) shows anticyclones along 25^{o} - 30^{o}N position and the associated ridge runs west-east. Easterly jet is observed at 15^{o}N with jet core wind of 50 knots.

b. Forecast wind

1-day forecast at 850 hPa (Fig. 3b) shows cyclonic circulation over NW India. The position of the circulation and that of the monsoon trough are to the south of the observed position. The cross-equatorial flow is predicted well. Strength of the low level jet is over estimated by 10-15 knots. The predicted positions of anticyclones along the equator are to the west of the observed position by 20^{o}. The associated ridge runs in the east-west direction.

In the 2-day forecast field at 850 hPa (Fig. 3c) the position of the cyclonic circulation over NW India is south of the 1-day predicted position. Other features are similar to that of the 1-day forecast. In the case of the 3-day forecast, at 850 hPa (Fig.3d) predicted position of the cyclonic circulation and monsoon

trough are further south of the 1- and 2-day predicted positions. Strength of the low level jet is 50 knots. The ridge along the equator runs north-west to south-east.

In all the forecast 1-, 2- and 3-day wind field at 200 hPa (Figs. 3f-h), the anticyclone to the north and the easterly jet are predicted well.

4.2 Spatial Distribution of wind error

The mean wind difference was computed by first finding the wind error (Forecast-Observed) of each 1-day,2-day and 3-day forecast and the corresponding observed wind and then averaging it for the month.

Mean zonal wind difference (Forecast-Observed) (Fig.4) for the 1-day forecast shows an intensification of the low level jet. Winds are over-estimated by 10 m s^{-1}.As the forecast progresses, the jet weakens and wind speed is 6 m s^{-1} for the 3-day forecast. The intensification of the low level jet seems to be spurious as the difference is reduced from 10 m s^{-1} to 6 m s^{-1} at the end of the 3-day forecast. This reduction could be attributed to the model adjustment in the course of integration. The error over the remaining area increases from the 1-day to the 3-day forecast.

The mean meridional wind difference (Fig. 5) shows that the strength of the cross-equatorial flow is over estimated by 6 m s^{-1} for the 1-day forecast. This error continues upto the 3-day forecast. Over the rest of the domain, the error increases from 4 m s^{-1} to 6 m s^{-1} as the forecast length increases from 1-day to 3-day. Over the Indian region the error is small-around 2 m s^{-1}.

4.3 Statistical scores

The quality of the model forecast is further examined by computing the following scores : RMS errors, standard deviation and absolute correlation for forecast and persistence. All the scores are computed for the wind field only.

a. RMS error

Fig. 6 shows the plots of mean RMSE of vector wind at 850, 500 and 200 hPa levels for forecast and persistence. It is clear from the figures that at 850 hPa level, persistence is superior to forecast. At 500 hPa level, forecast is found to be better than persistence. Same is the case of 200 hPa level which shows that, for the 1-day prediction, forecast and persistence are comparable whereas for the 2- and 3-day prediction, forecast is better than persistence.

b. Standard deviation (SD)

Fig.7 shows the daily variation of SD of vector wind error for 850 and 200 hPa levels. It can be seen from the figures that SD is minimum for 1-day forecast and maximum for 3-day forecast at 850 hPa indicating that, the forecast quality deteriorates as the forecast progresses. The 200 hPa level shows a similar pattern except for a few days when the 3-day forecast is better than the 2-day forecast.

c. Absolute correlation of vector wind for forecast and persistance

The correlation values (Table 1) indicate that except at 850 hPa level, forecast has an advantage over persistence at all the other levels for the 1-, 2- and 3-day prediction. This can be

distinctly seen at the mid-tropospheric levels where the difference in the correlation values is large indicating that forecast is better than persistence. This trend is also reflected in the vector wind RMSE (Fig. 6).

4.4 Rainfall

Total observed rainfall for July 1979 is shown in Fig.8. Data for the observed rainfall was collected from the Daily Rainfall Atlas (Krishnamurti et al. 1983), Rainfall values of each day was picked up from a 5^{o} x 5^{o} grid for the area 5^{o}N to 35^{o}N, 65^{o}E to 95^{o}E and then added for the whole month. The atlas provides rainfall analysis that include rain gauge as well as satellite observations. The total forecast rainfall for 1-, 2- and 3- day forecast is also shown in Fig. 8

a. Observed rainfall

Heavy rainfall is seen along the west coast with a maximum of 500 mm. Rainfall amount decreases as one goes towards the eastern coast where the values are below 200 mm. Another maximum of 400 mm can be seen in the north-eastern part of the country. NW India received rainfall between 50-150 mm while central India received around 250 mm of rainfall.

b. Forecast Rainfall

1-day forecast shows maximum rainfall of 300 mm in the Bay of Bengal. The position of this maximum is to the south of the observed position. Both the western as well as the eastern coasts

received less rainfall, the amounts being 50-100 mm and 100 mm respectively. NW India received rainfall between 50-100 mm, NE India between 150-200 mm and Central India around 150 mm.

The 2-day forecast does not show any maximum in the Bay of Bengal as seen in the 1-day forecast. Rainfall along the western coast is between 100-200 mm and a maximum 250 mm is seen in the Arabian Sea which is absent in the observed. NW India received rainfall around 100 mm while NE India and central India received between 150-200 mm.

In the 3-day forecast, rainfall along the west coast is around 150 mm while in the east coast it is 100 mm. NE, NW and Central India received around 100 mm of rainfall.

In general the rainfall rates are underpredicted. The 2-day forecast rainfall for all regions show the rainfall amounts to be greater than that of 1- and 3-day forecast. The 2-day forecast appears to be better while 3-day forecast is poor.

5. Conclusions

A nine-level limited area model has been used to produce 3-day forecasts using 31 successive days of July 1979 as input. Evaluation of the model forecasts revealed the following salient features :

i) In the mean wind field at 850 hPa, circulation features agree well with the observed though there is southward shifting of the cyclonic circulation over NW India and over estimation of the low level jet. At 200 hPa level forecast wind shows good agreement with the observed.

ii) Zonal wind error shows an intensification of the low

level jet in the 1-day forecast which subsequently weakens by the end of the 3-day forecast. The error is probably spurious and its reduction can be attributed to the model adjustment during the course of integration. The meridional wind error is small over the Indian region while in the remaining domain error grows with time. Strength of the cross-equatorial flow is over estimated by 6 m s^{-1} for all the 3-day forecasts.

iii) Mean RMSE as well as absolute correlation of vector wind shows forecast to be superior to persistence at all levels except at 850 hPa level. Standard deviation indicates deterioration of forecast quality as the forecast progresses.

iv) Rainfall rates are predicted to be much less than the observed. The 2-day forecast appears better while the 3-day forecast is poor.

Acknowledgements

Authors are thankful to Prof. R.N. Keshavamurty, Director, Indian Institute of Tropical Meteorology for his keen interest in the study.

REFERENCES

Anthes R.A. 1977 : A Cumulus parameterization scheme utilisin a one-dimensional cloud model.Mon.Wea.Rev. 105 ,270-286.

Arakawa, A. and Mintz, Y. 1974 : The UCLA Atmospheric General Circula tion Model (with the participation of K. Katayama, J.W. Kim W. Schubert, T. Tokioka, M. Schlesinger, W.Chao,D. Randall an L. Lord). Notes distributed at the Workshop,25 March-4 Apri 1974, Department of Meteorology, University of California.

Kondo,J. 1975 : Air-sea bulk transfer coefficients in diabati conditions. Bound.Layer Met. , 9 , 91-112.

Krishnamurti, T.N., Steven Cocke, Richard Pasch, Simon Low-Nam, 1983 : Precipitation estimates from raingauge and satellite observations Summer MONEX, FSU report no. 83-7.

Kuo, H.L., 1974 : Further studies of the parameterization of the influence of cumulus convection on large scale flow. J.Atmos. Sci., 31, 1232-1240.

Perkey, D.J. and Kreitzberg, 1976 : A time-dependent lateral boundary scheme for limited area primitive equation model. Mon.Wea.Rev., 104, 744-755.

Rajagopal, E.N. and S.S. Singh, 1991 : Cumulus convection and lateral boundary conditions. Proceedings Indian Academy of Sciences (Earth & Planetary Sciences), 100, 235-253.

Sasaki, Y.K., Ray, P.S., Goerss, J.S. and Soliz, P., 1979: Inconsistent finite differencing errors in the variational adjustment of horizontal wind components. J.Met.Soc. of Japan, 59, 88-92.

Singh, S.S., S.S. Vaidya and E.N. Rajagopal, 1990 : A limited area model for monsoon prediction. Advances in Atmos. Sci., 7, 111-126.

Tatsumi, Y., 1983 : An economical explicit time integration scheme for a primitive model. J.Met.Soc. of Japan, 61, 269- 289.

Table 1 : Absolute correlation of vector wind for Forecast (F) and Persistence (P)

FORECAST	1-DAY		2-DAY		3-DAY	
LEVEL	F	P	F	P	F	P
850	0.88	0.91	0.83	0.84	0.80	0.81
700	0.86	0.81	0.81	0.69	0.77	0.62
500	0.81	0.69	0.75	0.47	0.70	0.33
400	0.81	0.73	0.74	0.55	0.70	0.45
300	0.84	0.79	0.78	0.67	0.76	0.62
250	0.85	0.81	0.80	0.71	0.79	0.67
200	0.83	0.82	0.79	0.74	0.78	0.69

LEGENDS OF FIGURES

Fig. 1 : Vertical structure of the model

Fig. 2 : Horizontal staggering

Fig.3a : 850 hPa Mean observed wind (Isotachs in knots)

Fig.3b : 850 hPa Mean wind 1-day forecast (Isotachs in knots)

Fig.3c : 850 hPa Mean wind 2-day forecast (Isotachs in knots)

Fig.3d : 850 hPa Mean wind 3-day forecast (Isotachs in knots)

Fig.3e : 200 hPa Mean observed wind (Isotachs in knots)

Fig.3f : 200 hPa Mean wind 1-day forecast (Isotachs in knots)

Fig.3g : 200 hPa Mean wind 2-day forecast (Isotachs in knots)

Fig.3h : 200 hPa Mean wind 3-day forecast (Isotachs in knots)

Fig. 4 : 850 hPa Mean Zonal Wind difference (ms^{-1})

Fig. 5 : 850 hPa Mean meridional wind difference (ms^{-1})

Fig. 6 : Mean RMSE of vector wind (ms^{-1})

Fig. 7 : Standard deviation of wind error (ms^{-1})

Fig. 8 : Total rainfall (mm) - July 1979

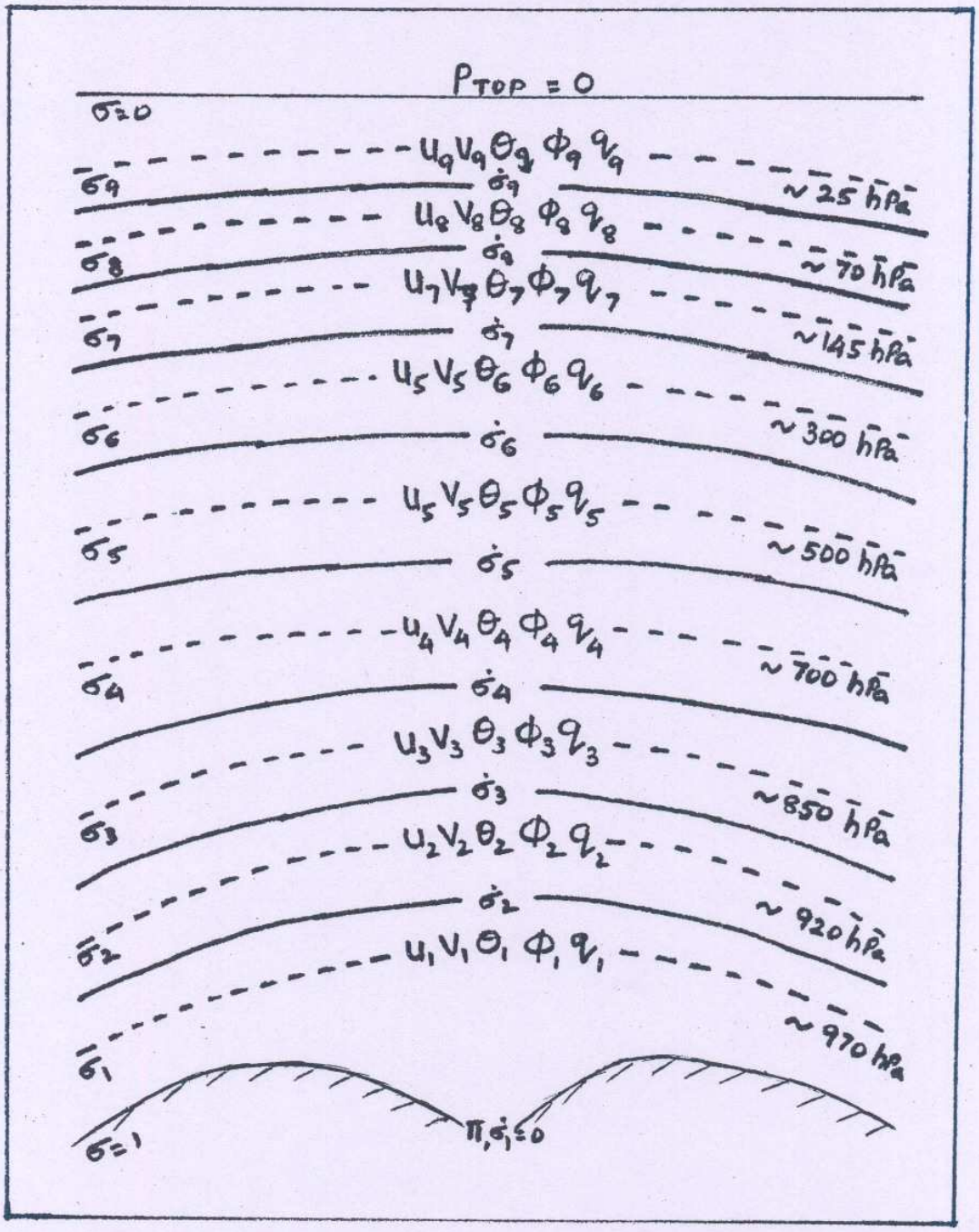

Fig 1: Vertical structure of the model

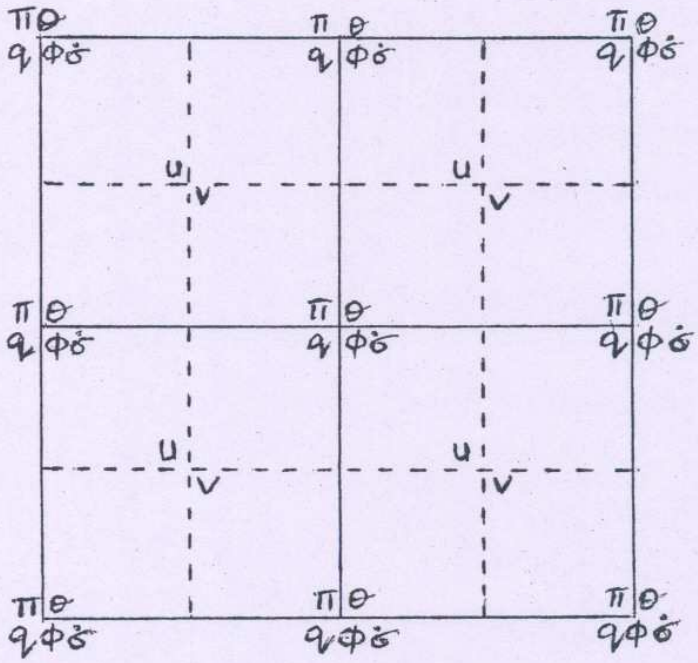

Fig 2 : Horizontal staggering

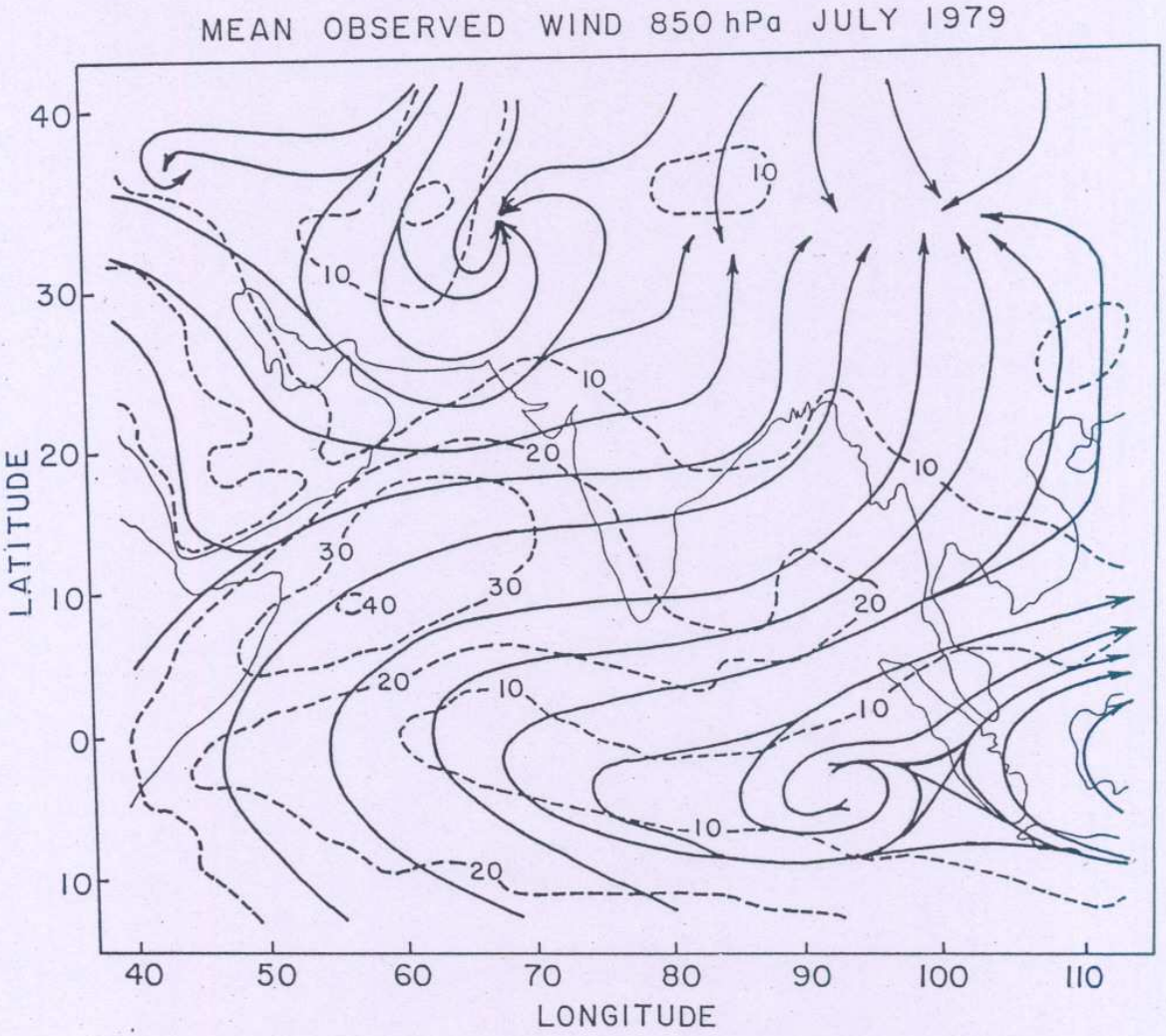
MEAN OBSERVED WIND 850 hPa JULY 1979
LATITUDE
LONGITUDE
40
30
20
10
0
10
40
50
60
70
80
90
100
110
10
20
30
40

Fig. 3a

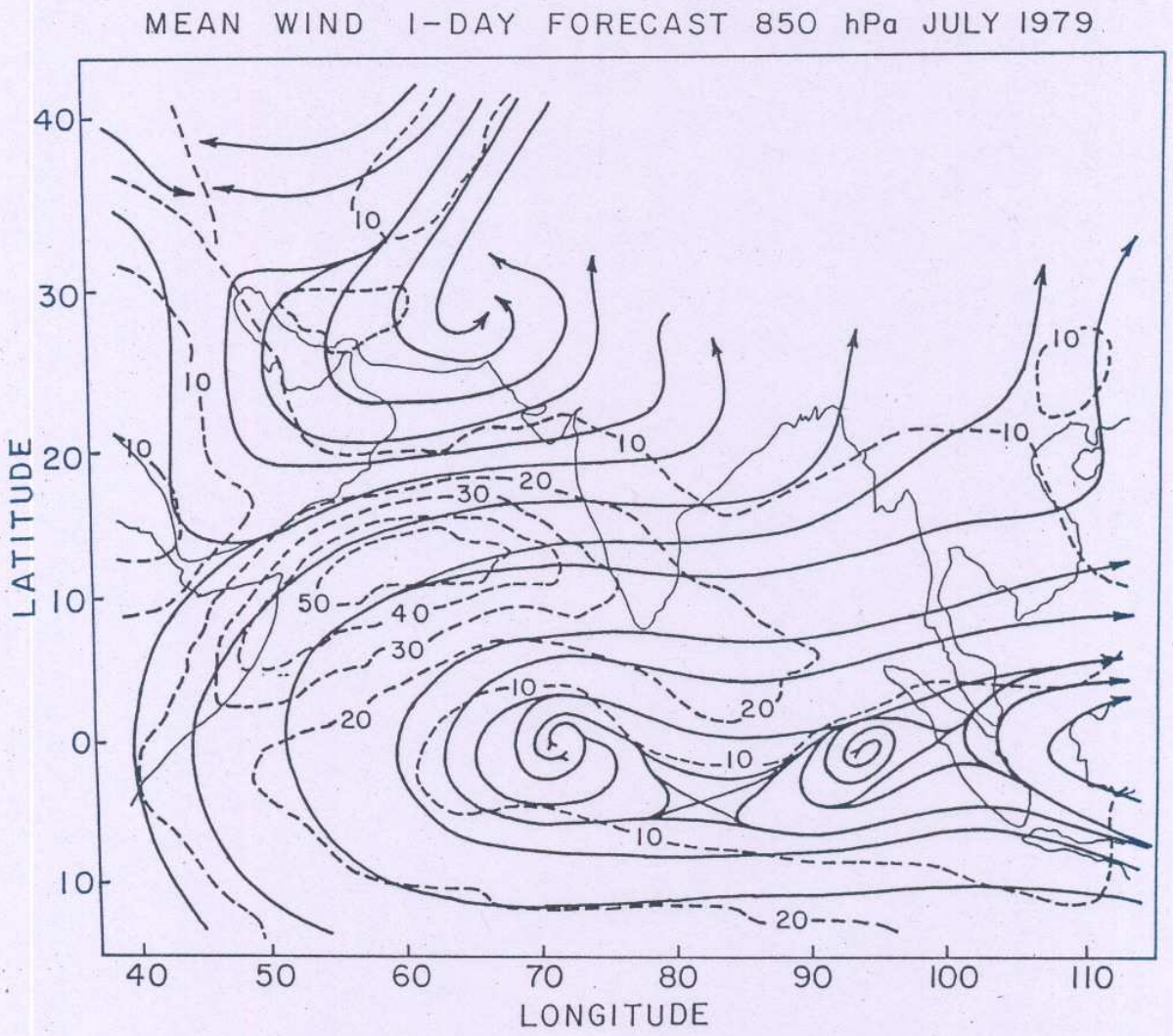
MEAN WIND 1-DAY FORECAST 850 hPa JULY 1979
LATITUDE
LONGITUDE
40
30
20
10
0
10
40
50
60
70
80
90
100
110
10
10
10
10
10
10
10
10
10
10
20
20
20
20
30
30
40
50

Fig. 3b

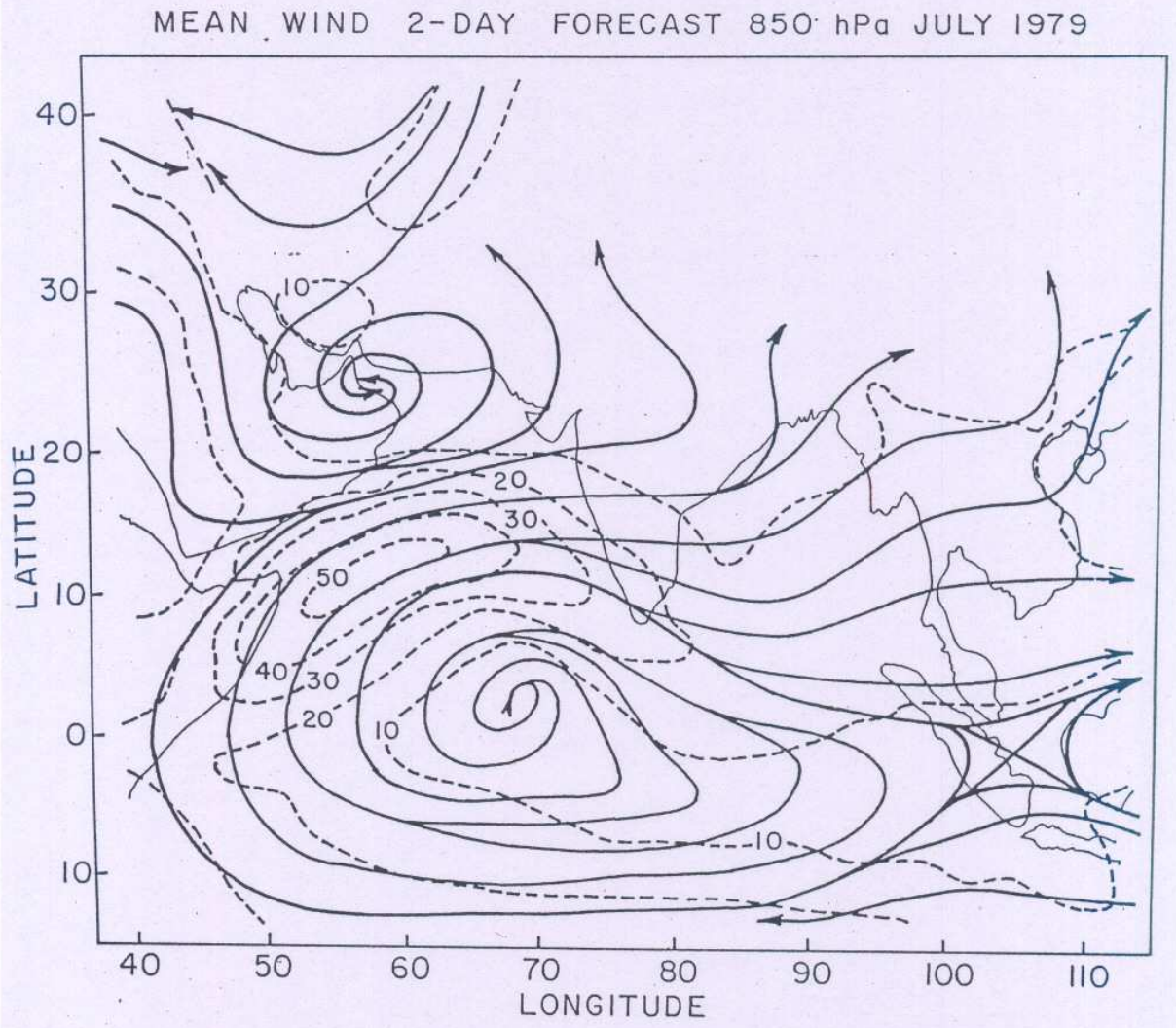
MEAN WIND 2-DAY FORECAST 850 hPa JULY 1979
LATITUDE
LONGITUDE
40
30
20
10
0
10
40
50
60
70
80
90
100
110
10
20
30
50
40
30
20
10
10

Fig. 3c

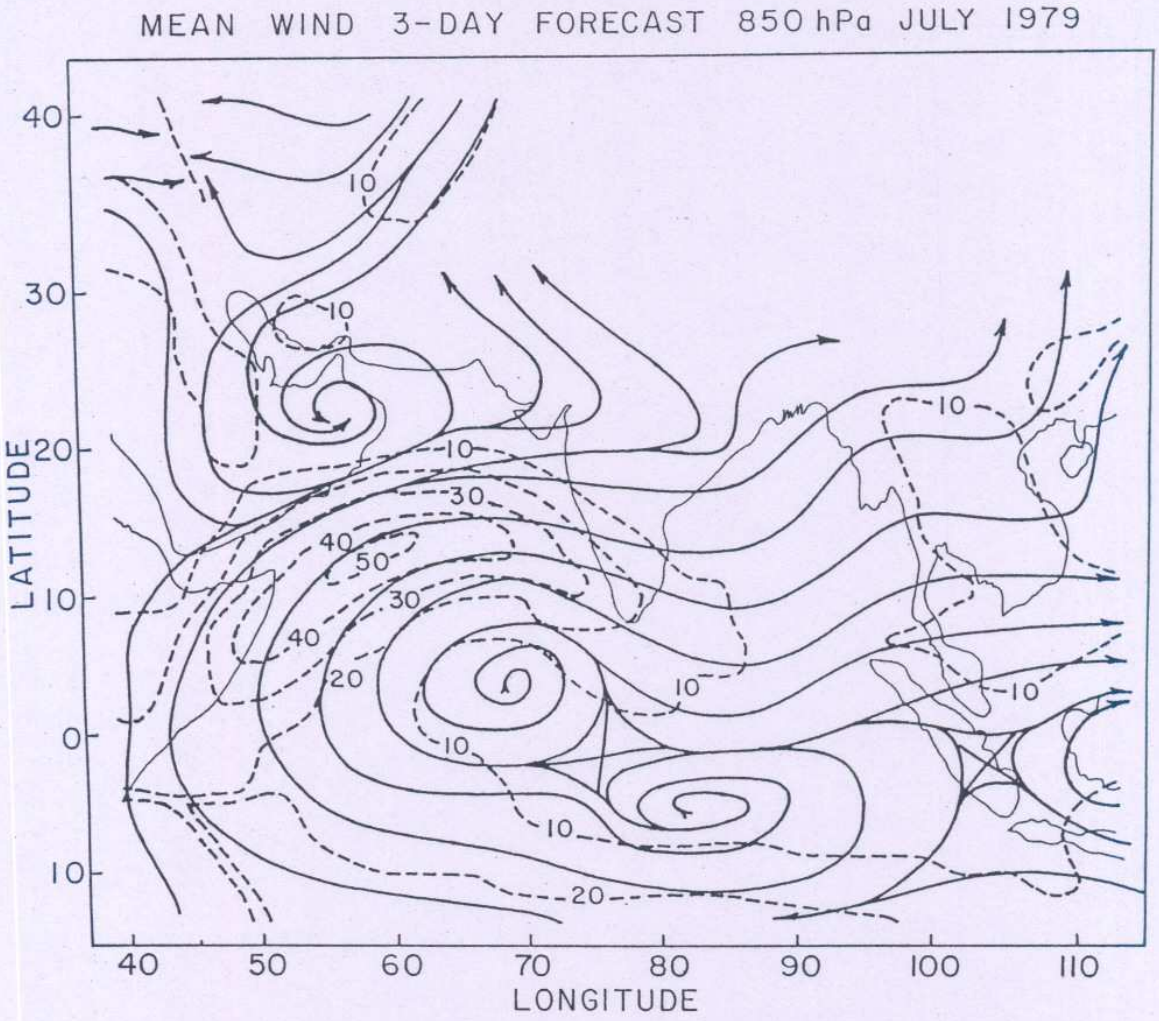
MEAN WIND 3-DAY FORECAST 850 hPa JULY 1979
LATITUDE
LONGITUDE
40
30
20
10
0
10
40
50
60
70
80
90
100
110
10
10
10
30
40
50
30
40
20
10
10
10
10
10
10
20

Fig. 3d

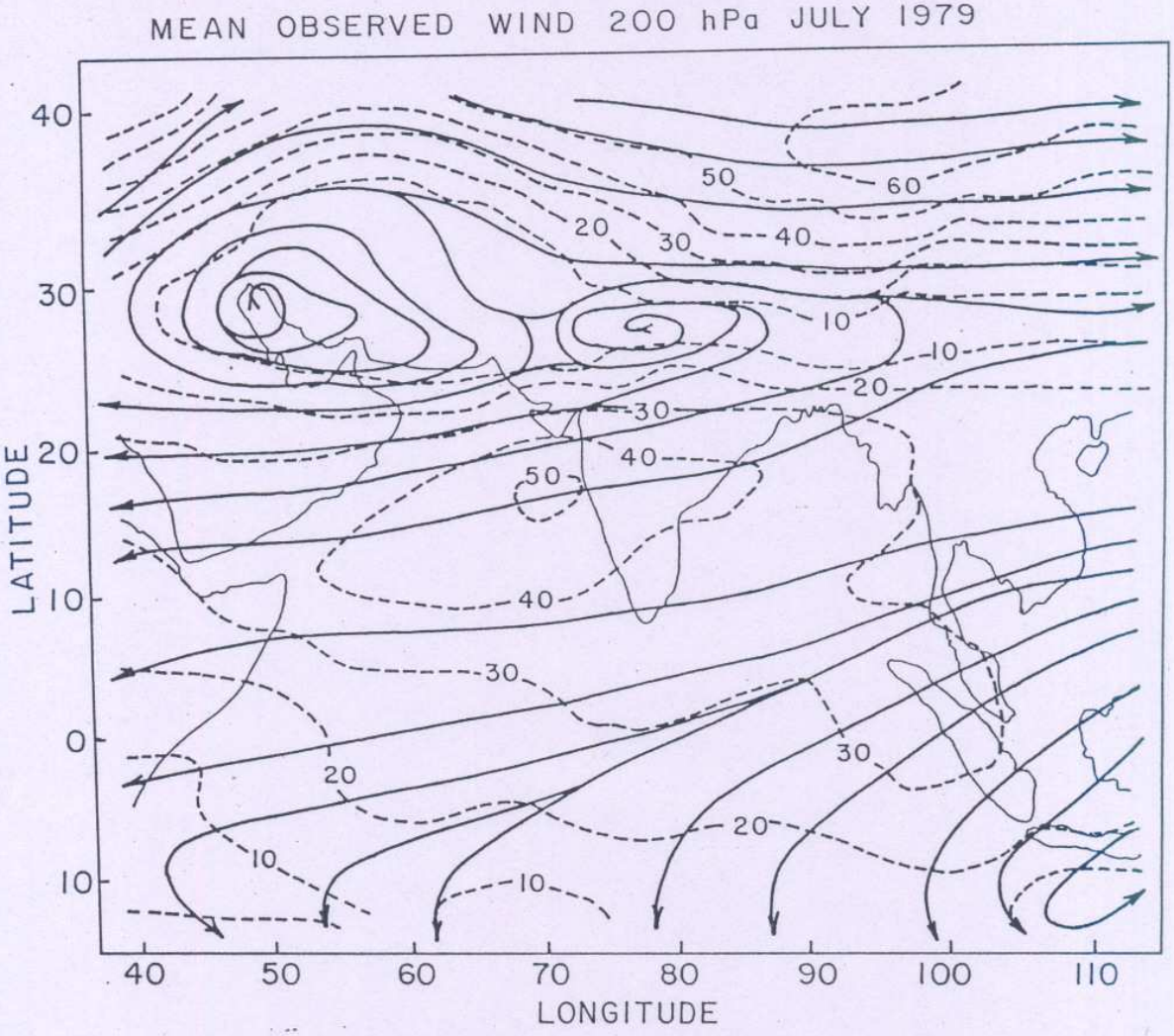
MEAN OBSERVED WIND 200 hPa JULY 1979
LATITUDE
LONGITUDE
40
30
20
10
0
10
40
50
60
70
80
90
100
110
50
60
20
30
40
10
10
20
30
40
50
40
30
20
30
20
10
10

Fig. 3e

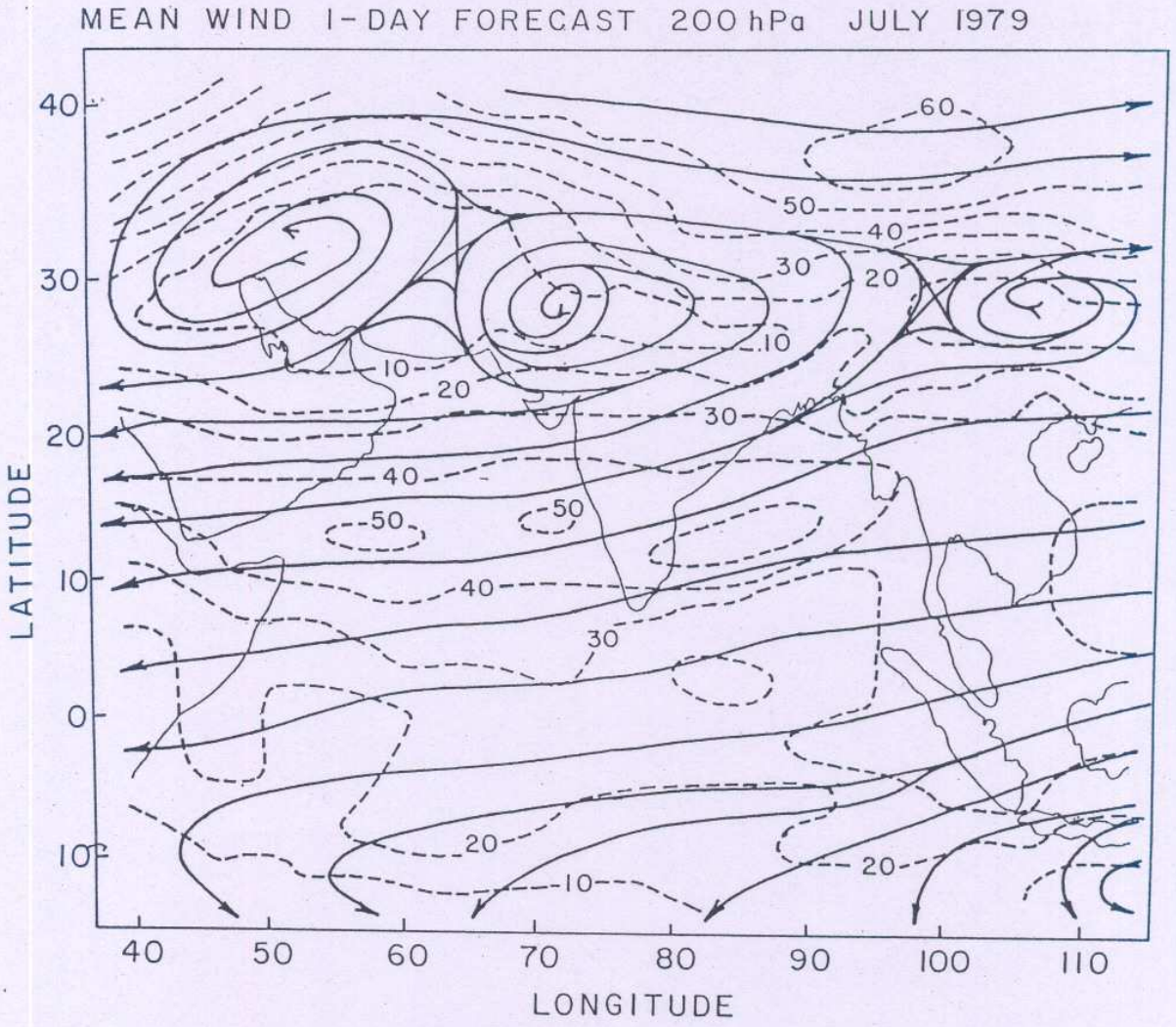
MEAN WIND 1-DAY FORECAST 200 hPa JULY 1979
LATITUDE
LONGITUDE
40
30
20
10
0
10
40
50
60
70
80
90
100
110
60
50
40
30
20
10
10
20
30
40
50
50
40
30
20
10
20

Fig. 3f

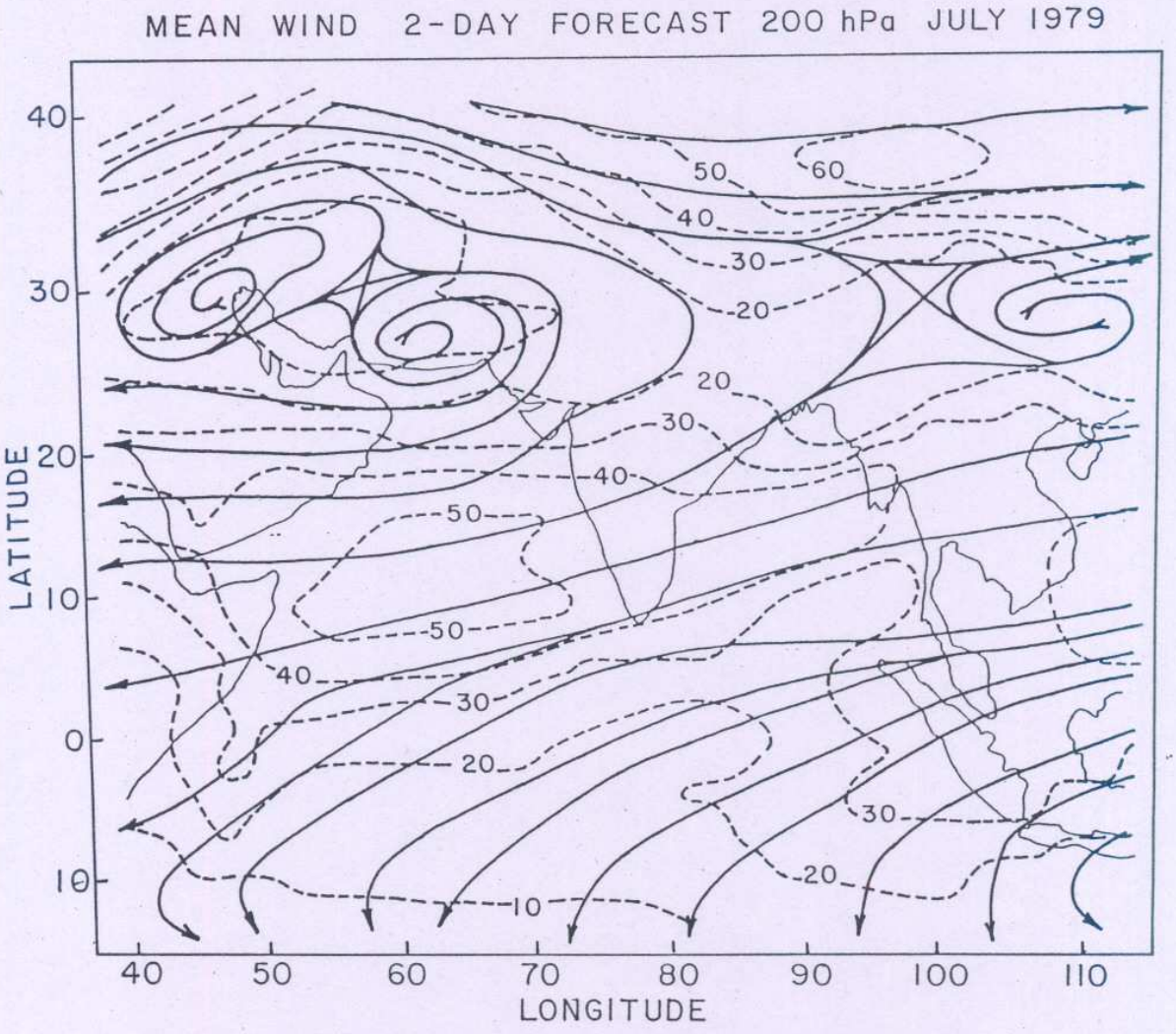
MEAN WIND 2-DAY FORECAST 200 hPa JULY 1979
LATITUDE
LONGITUDE
40
30
20
10
0
10
40
50
60
70
80
90
100
110
50
60
40
30
20
20
30
40
50
50
40
30
20
30
20
10

Fig. 3g

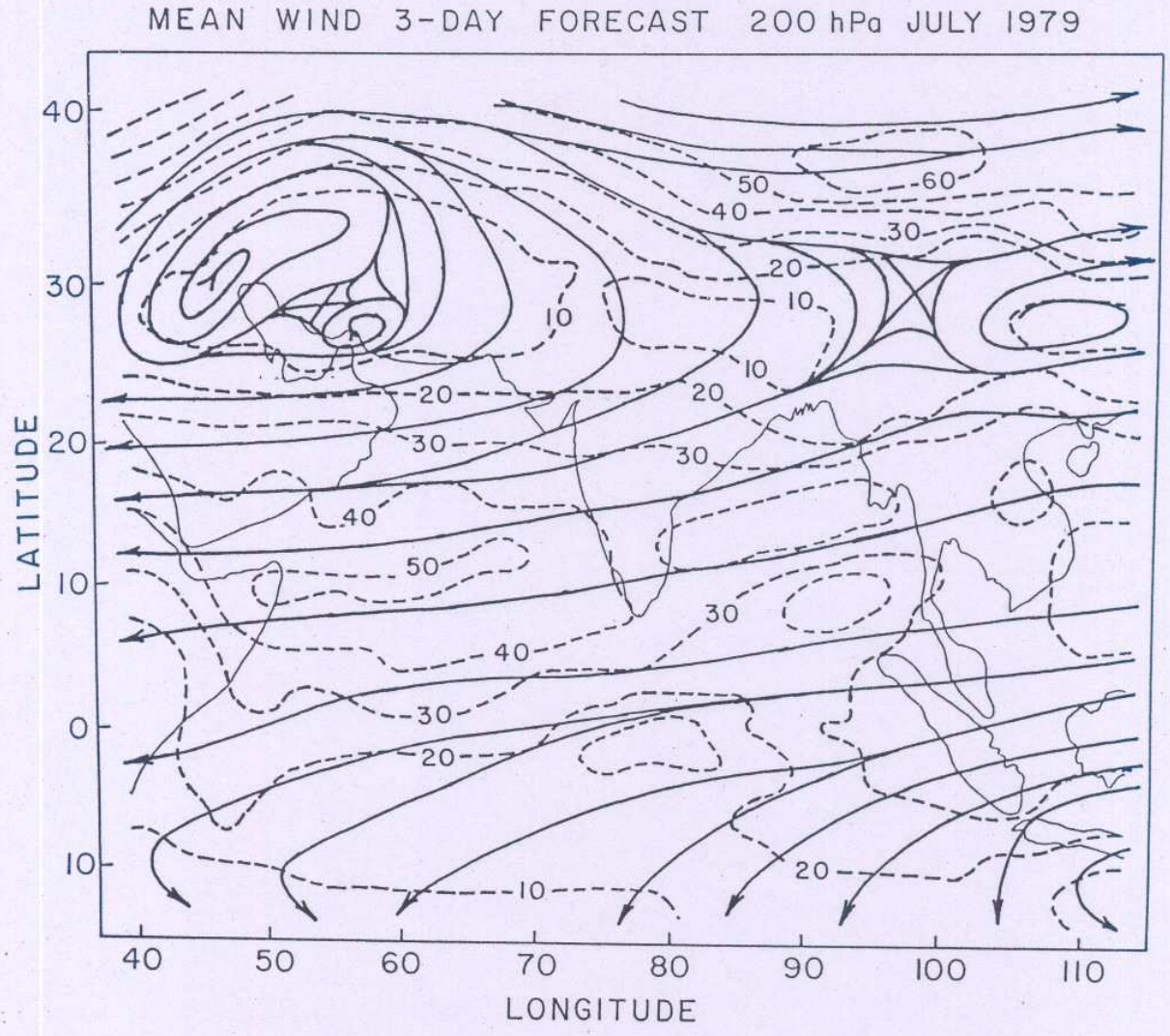
MEAN WIND 3-DAY FORECAST 200 hPa JULY 1979
LATITUDE
LONGITUDE
40
30
20
10
0
10
40
50
60
70
80
90
100
110
10
20
30
40
50
60

Fig. 3h

1-DAY FORECAST

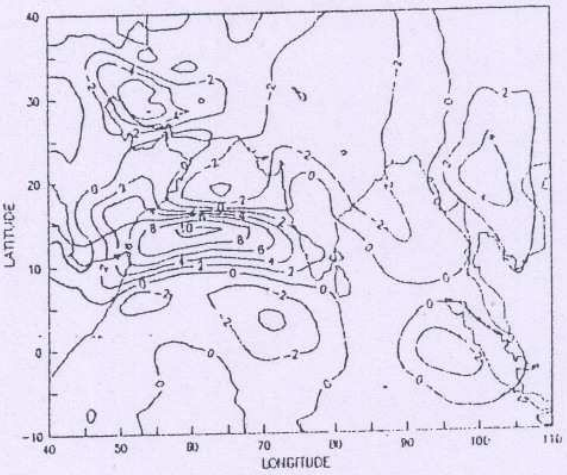

2-DAY FORECAST

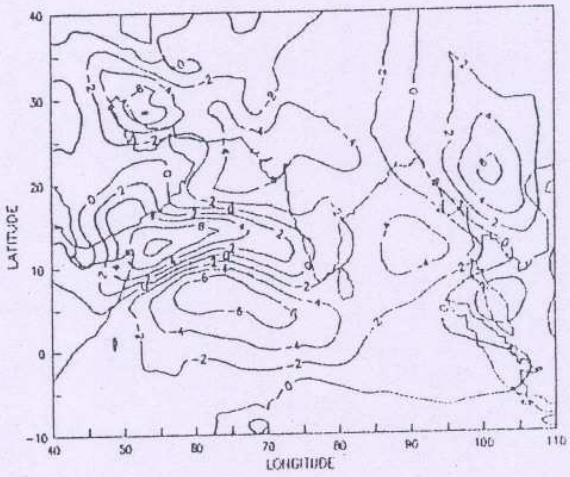

3-DAY FORECAST

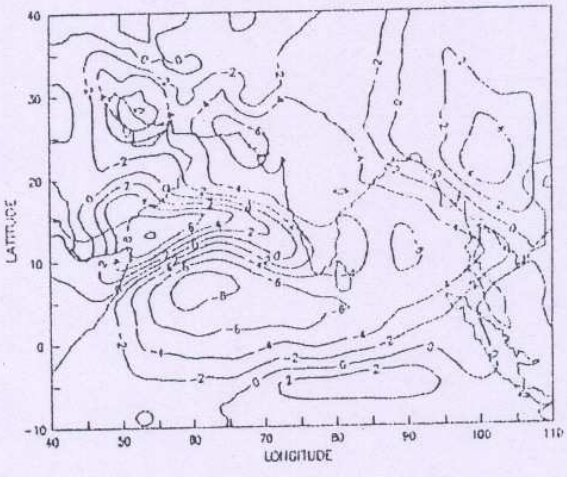

Fig. 4

1-DAY FORECAST

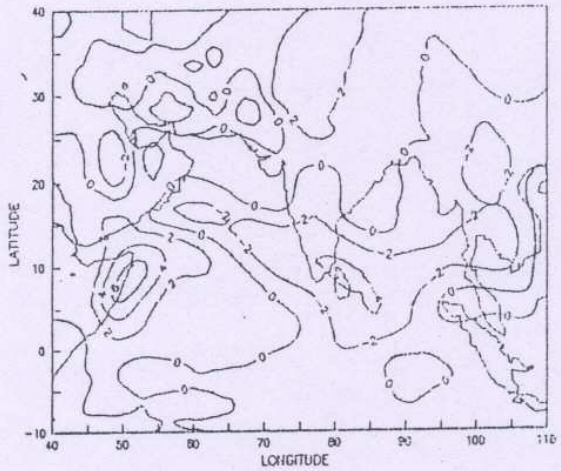

2-DAY FORECAST

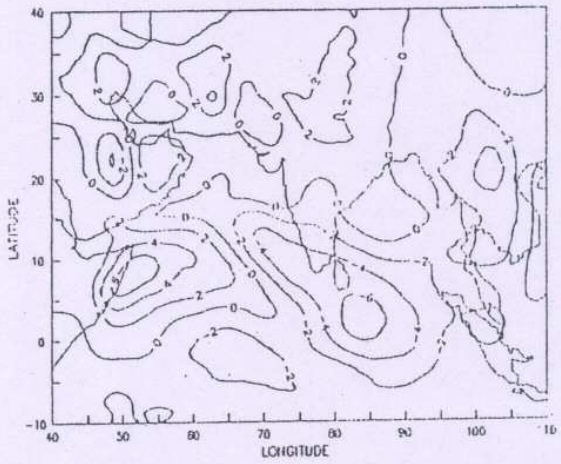

3-DAY FORECAST

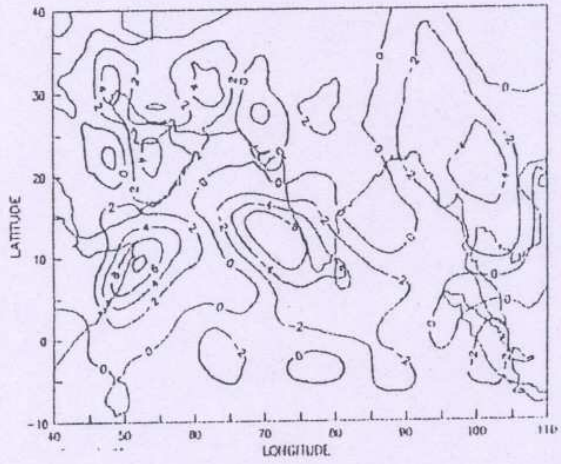

Fig. 5

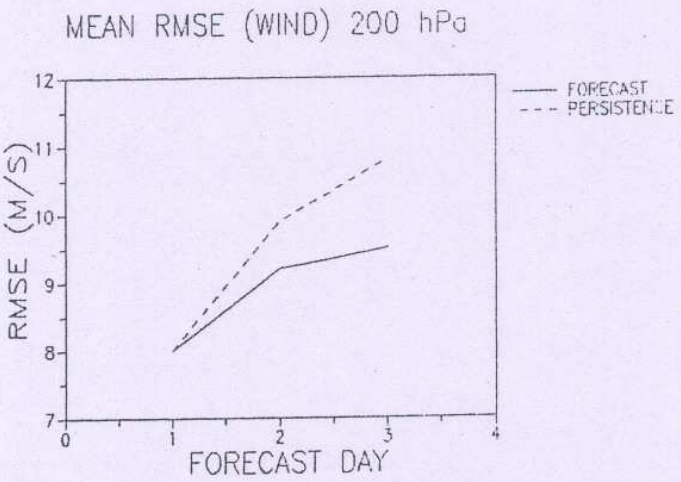
MEAN RMSE (WIND) 200 hPa
FORECAST
PERSISTENCE
RMSE (M/S)
12
11
10
9
8
7
0
1
2
3
4
FORECAST DAY

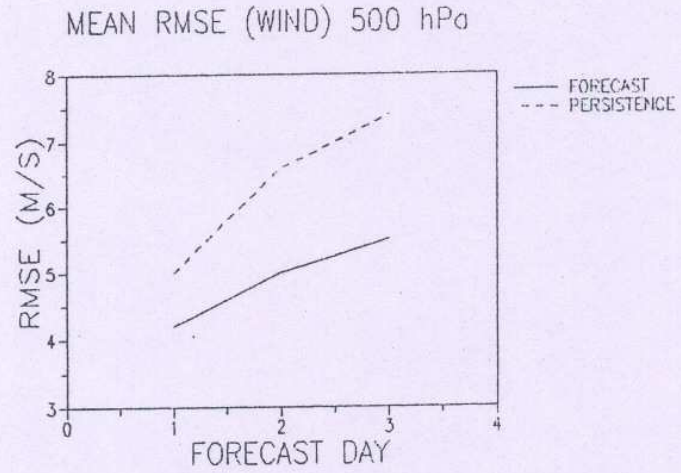
MEAN RMSE (WIND) 500 hPa
FORECAST
PERSISTENCE
RMSE (M/S)
8
7
6
5
4
3
0
1
2
3
4
FORECAST DAY

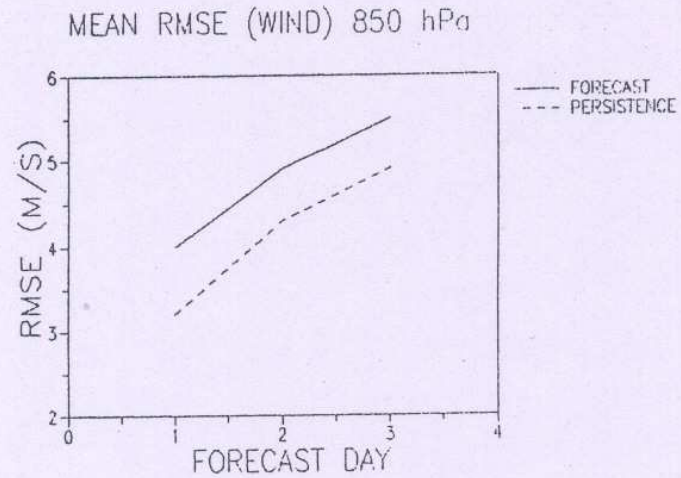
MEAN RMSE (WIND) 850 hPa
FORECAST
PERSISTENCE
RMSE (M/S)
6
5
4
3
2
0
1
2
3
4
FORECAST DAY

Fig. 6

STANDARD DEVIATION OF WIND ERROR 200 hPa

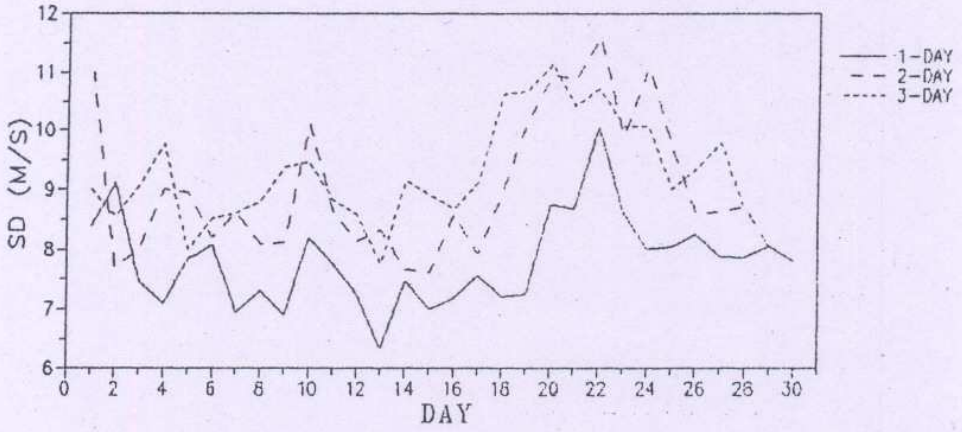

STANDARD DEVIATION OF WIND ERROR 850 hPa

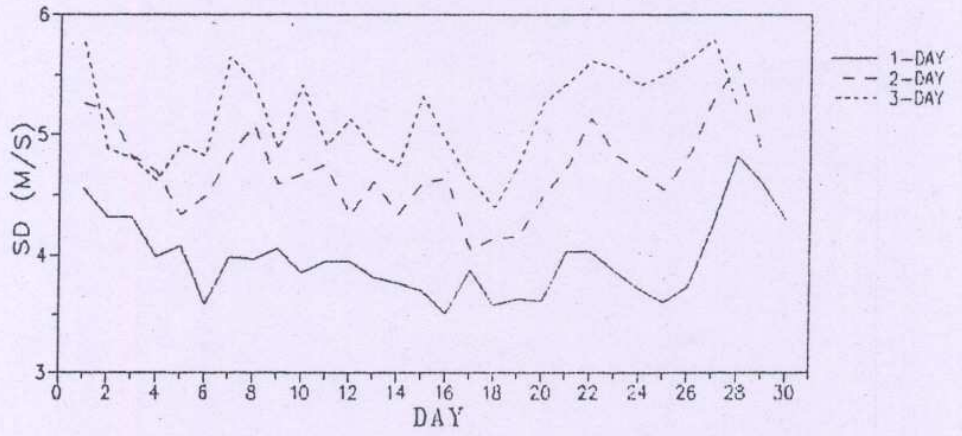

Fig. 7

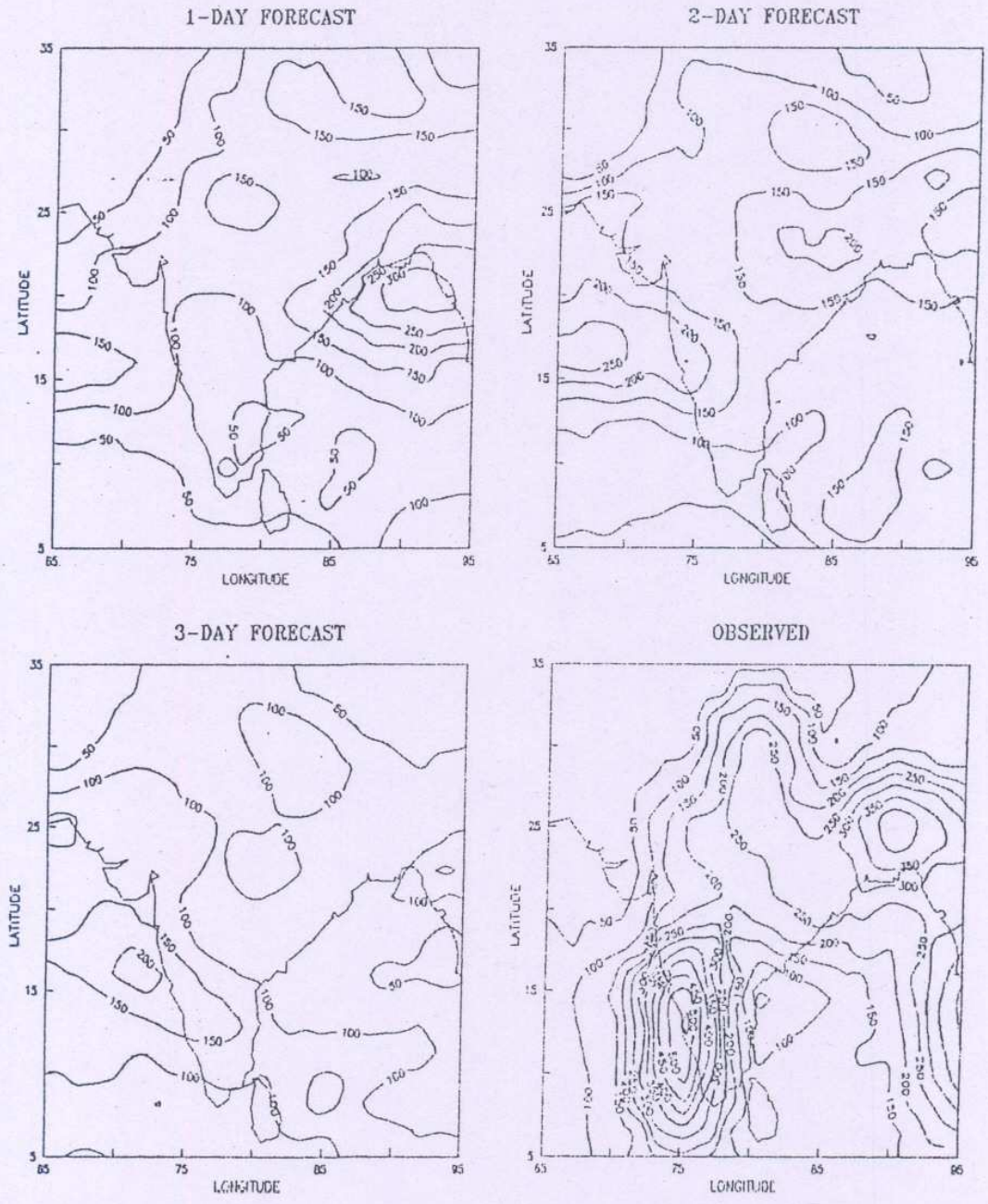

Fig. 8

प्रत्यक्ष सत्यापित

P. V. 1999-2000